Non-Iris Occlusions Detection

Michal Haindl Mikuláš Krupička
Institute of Information Theory and Automation of the ASCR
182 08 Prague, Czech Republic

Faculty of Information Technology, Czech Technical University
160 00 Prague, Czech Republic
haindl@utia.cas.cz, krupimik@fit.cvut.cz

Abstract

The prerequisite for the accurate iris recognition is to detect all iris occlusions which would otherwise confuse a recognition method and impair its recognition rate. This paper presents a fast multispectral eyelid, eyelash, and reflection detection method based on the underlying three-dimensional spatial probabilistic textural model. The model first adaptively learns its parameters on the flawless iris texture part and subsequently checks for non iris occlusions using the recursive prediction analysis. We provide colour iris occlusion detection results that indicate the advantages of the proposed method and compare it with 97 recent Noisy Iris Challenge Evaluation algorithms.

1. Introduction

Biometrics based human identification systems have ever growing importance in recent trends towards more secure modern information society. Biometrics recognition systems are not only widespread in various security applications such bank access, airport entry points, or criminal evidence gathering but also for smart homes or cars control or handicapped help systems. Various biometric data can be exploited for these applications. It can be human voice, fingerprint, eye, face, gait, veins, handwriting and many more. Various biometric data differ in ways how to acquire them, their durability, reliability, safety, and necessary technology for their acquisition and evaluation. In this work we focus on iris recognition because of its stability over man's life, ease of acquisition (can be acquired remotely from distance of up to several meters), and accuracy. The possibility for the eye-based human identification was originally suggested by [1] and later estimated that the probability of two similar iris is 1 in 10^{72} [24]. For a survey of the iris recognition results see [2].

The iris identification is complex task containing several sub-tasks (see the processing schema on Fig.1) that have to be solved. The whole process starts with image acquisition which hardly produces ideal noise-free, focused, and homogeneously illuminated images, thus the corresponding preprocessing steps for data normalization, denoising, or geometric corrections are inevitable before the iris segmentation can be performed. The iris segmentation results are typically coordinates of two circles, inner and outer border of iris. Additionally, a normalization step has been introduced to simplify the subsequent processing steps. Normalization is usually done transforming the iris into a fixed size rectangle. The selected features are then computed from the normalized rectangle and used in a classifier to recognize a corresponding human.

Unconstrained iris measurements contain numerous occlusion defects such as eyelid, eyelash, and reflections which have to be detected in the preprocessing step of any iris recognition algorithm. Otherwise such occlusions would confuse the recognition method and impair its recognition rate. Although such unconstrained visible wavelength iris image acquisition impose minimal constraints on the iris verification and identification process as well as on the subject [3], hence allowing wider range of possible iris recognition applications, it obviously requires more demanding iris processing methods to achieve comparable recognition rate with the rigid optimal acquisition conditions (homogeneous fixed illumination, direct, close, and fixed distance look to the sensor).

1.1. Non-Iris Overlaps Detection

Due to the various iris imperfections which are often found on unconstrained iris measurements, such as reflections, upper and lower eyelids, eyelid shadows, or eyelashes, iris classifiers performance have insufficient reliability. Thus it is necessary to remove such areas from the iris texture prior to the classification process what constitutes on of the most challenging problem in the iris recog-

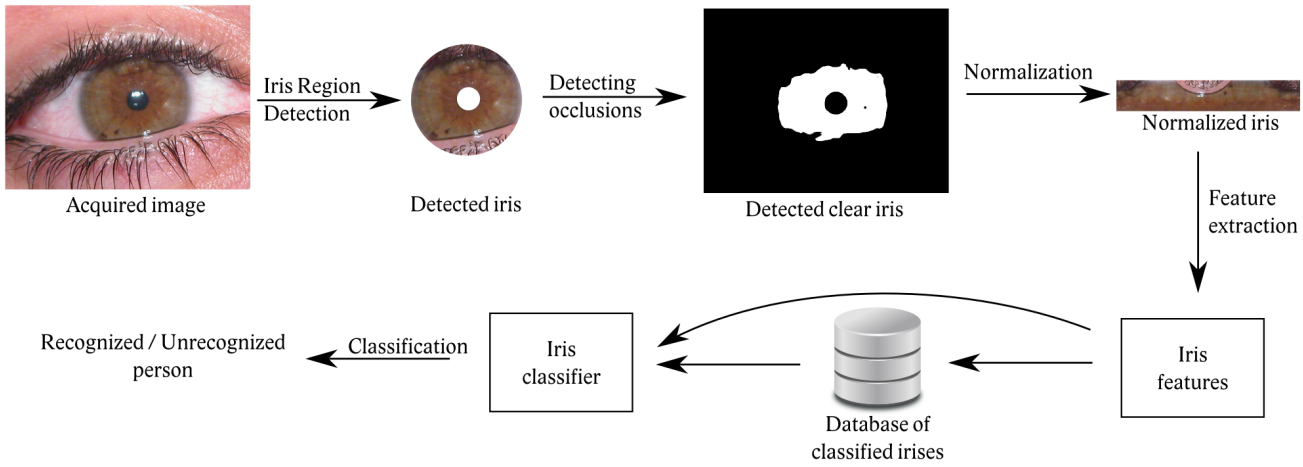

Figure 1. Iris recognition processing pipeline .

nition research [24]. Some detection methods are specialized to single imperfection category only, while others [3, 7, 14, 17, 18, 19, 27, 28, 31] can detect several types of imperfections.

Methods focused only on reflections are based on (adaptive) thresholding (eg. [29]). Thresholding is very fast approach with decent results but typical problem are glasses or contact lenses (with large reflectors). Typical eyelid detectors are based on edge detection followed with polynomial fitting (eg. [8, 32]). Chen *et al.* [4] proposed method of eyelash detection based on simple thresholding but claims that result quality highly depends on chosen image capture device. He *et al.* [13] proposed similar method (applicable also on eyelid shadow) with threshold value based on a statistical prediction model. One of the first general imperfection detection methods was presented by Proenca [27]. This method is based on training classifier on manually detected irises. The eye representation is based on textural GLCM [12] features and the detector uses a neural network classifier.

The conventional approach for defect detection [5] is to compute a texture features in a local sub-window and to compare them with the reference values representing a perfect pattern. The method [20] preprocesses a gray level textile texture with histogram modification and median filtering. The image is subsequently thresholded using the adaptive filter and finally smoothed with another median filter run. Another approach for detection of gray level textured defects using linear FIR filters with optimized energy separation was proposed in [16]. Similarly the defect detection [30] is based on a set of optimized filters applied to wavelet sub-bands and tuned for a defect type. Method [9] uses translation invariant 2D RI-Spline wavelets for textile surface inspection. The gray level texture is removed using the wavelet shrinkage approach and defects are subsequently detected by simple thresholding. Contrary to above approaches the presented method uses the visible wavelength multispectral information.

Recent state-of-the-art non-iris occlusions detectors were mostly competing in the 2008 NICE.I (Noisy Iris Challenge Evaluation) focusing especially on detection accuracy. Nearly hundred various methods from 22 countries were submitted to this challenge and the best-ranked algorithms were published in [23]. The presented method uses these best-ranked algorithms for comparison. Anyhow, contrary to our method none of these NICE methods use true multispectral information. The source images (which are in RGB colour space) are typically either converted to greyscale before any analytical steps or only one spectrum channel is used. The best method by Tan et al. [31] uses clustering for iris localization followed with prediction and curvature models for eyelid and eyelash detection. The second best method by Sankowski et al.[28] consists of three steps - threshold based reflections detection, iris boundaries detection based on modified integro-differential operator, and eyelids detection based on parametric modelling. The third method by Pedro Almeida [7] is based on an expert system with set of decision rules which mainly present novel iris boundary detection and upper and lower eyelid arc fitting. Finally, the fourth method by Jeong et al. [14] uses K-Means clustering in the co-occurrence histogram for iris boundaries detection followed with upper and lower eyelid detection based on the fitting model of parabolic integro-differential operator.

The organization of this paper is as follows. First, a concise description of the underlying 3D multispectral texture model as well as the model selection criterion is given. The third section summarizes the core part of the detection algorithm followed by the experimental results and conclusions sections.

2. Multispectral Iris Texture Model

We assume that the multispectral iris texture can be represented by an adaptive 3D causal simultaneous autoregressive model [10, 11]:

$$X_r = \sum_{s \in I_r^c} A_s X_{r-s} + \epsilon_r \ , \tag{1}$$

where ϵ_r is a white Gaussian noise vector with zero mean, and a constant but unknown covariance matrix Σ and $r = \{r_1, r_2\}, s = \{s_1, s_2\}$ are multiindices with the row and column indices, respectively. The noise vector is uncorrelated with data from a causal neighbourhood I_r^c,

$$A_{s_1,s_2} = \begin{pmatrix} a_{1,1}^{s_1,s_2}, \ldots, a_{1,d}^{s_1,s_2} \\ \vdots, \ddots, \vdots \\ a_{d,1}^{s_1,s_2}, \ldots, a_{d,d}^{s_1,s_2} \end{pmatrix} \tag{2}$$

are $d \times d$ parameter matrices where d is the number of spectral bands. $r, r-1, \ldots$ is a chosen direction of movement on the image lattice (e.g. scanning lines rightward and top to down). This model can be analytically estimated using numerically robust recursive statistics hence it is exceptionally well suited for possibly real-time texture defect detection applications. The model adaptivity is introduced using the standard exponential forgetting factor technique in the parameter learning part of the algorithm. The model can be alternatively written in the matrix form

$$X_r = \gamma Z_r + \epsilon_r \ , \tag{3}$$

where $\gamma = [\, A_1, \ldots, A_\eta]$, $\eta = card(I_r^c)$ is a $d \times d\eta$ parameter matrix and Z_r is a corresponding vector of X_{r-s}. To evaluate the conditional mean values $E\{X_r \,|\, X^{(r-1)}\}$, where $X^{(r-1)}$ is the past process history, the one-step-ahead prediction posterior density $p(X_r \,|\, X^{(r-1)})$ is needed. If we assume the normal-gamma parameter prior for parameters in (1) this posterior density has the form of Student's probability density with $\beta(r) - d\eta + 2$ degrees of freedom, where the following notation is used:

$$\begin{aligned} \beta(r) &= \beta(0) + r - 1 \ , && (4) \\ \hat{\gamma}_{r-1}^T &= V_{zz(r-1)}^{-1} V_{zx(r-1)} \ , && (5) \\ V_{r-1} &= \begin{pmatrix} \tilde{V}_{xx(r-1)} & \tilde{V}_{zx(r-1)}^T \\ \tilde{V}_{zx(r-1)} & \tilde{V}_{zz(r-1)} \end{pmatrix} + I \ , && (6) \\ \tilde{V}_{uw(r-1)} &= \sum_{k=1}^{r-1} U_k W_k^T \ , && (7) \\ \lambda_{(r)} &= V_{x(r)} - V_{zx(r)}^T V_{z(r)}^{-1} V_{zx(r)} \ , && (8) \end{aligned}$$

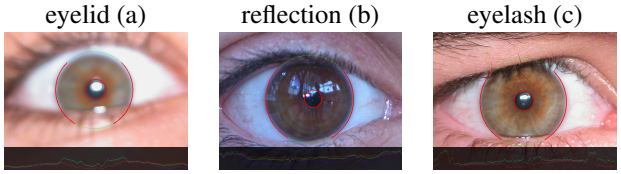

Figure 2. Detected iris regions containing all three (a,b,c) occlusion types.

where $\beta(0) > 1$ and U, W denote either X or Z vector, respectively. If $\beta(r-1) > \eta$ then the conditional mean value is

$$E\{X_r | X^{(r-1)}\} = \hat{\gamma}_{r-1} Z_r \tag{9}$$

and it can be efficiently computed using the following recursion

$$\hat{\gamma}_r^T = \hat{\gamma}_{r-1}^T + \frac{V_{z(r-1)}^{-1} Z_r (X_r - \hat{\gamma}_{r-1} Z_r)^T}{1 + Z_r^T V_{z(r-1)}^{-1} Z_r} \ . \tag{10}$$

The selection of an appropriate model support (I_r^c) is important to obtain good iris representation. If the contextual neighbourhood is too small it can not capture all details of the random field iris model. Inclusion of the unnecessary neighbours on the other hand adds to the computational burden and can potentially degrade the performance of the model as an additional source of noise. The optimal Bayesian decision rule for minimizing the average probability of decision error chooses the maximum posterior probability model, i.e., a model M_i corresponding to

$$\max_j \{p(M_j | X^{(r-1)})\}$$

can be found analytically [10, 11].

3. Defect Detection

The eye area is found using the integro-differential Daugman operator [6]. Single multispectral pixels are classified as belonging to the defective (non-iris) area based on their corresponding prediction errors. If the prediction error is larger than the adaptive threshold:

$$\begin{aligned} &|\tilde{E}\{X_r \,|\, X^{(r-1)}\} - X_r| > \\ &\frac{\alpha}{l} \sum_{i=1}^{l} \left| \tilde{E}\{X_{r-i} \,|\, X^{(r-i-1)}\} - X_{r-i} \right| \ , \end{aligned} \tag{11}$$

then the pixel r is classified as a detected defect pixel. The parameter l in (12) is a process history length of the adaptive threshold and the constant $\alpha = 2.7$ was found experimentally.

The one-step-ahead predictor

$$\tilde{E}\{X_r \mid X^{(r-1)}\} = \hat{\gamma}_s \, Z_r \tag{12}$$

differs from the corresponding predictor (9) in using parameters $\hat{\gamma}_s$ which were learned only in the flawless texture area ($s < r$). The small learning flawless texture cutout is found automatically inside reflection-less iris area. The whole algorithm is extremely fast because the adaptive threshold is updated recursively:

$$|\epsilon_{r+1}| > \frac{\alpha}{l} \left[\sum_{i=0}^{l-1} |\epsilon_{r-i}| \right] \quad , \tag{13}$$

where ϵ_r is the prediction error

$$\epsilon_r = \tilde{E}\{X_r \mid X^{(r-1)}\} - X_r \quad ,$$

and $\hat{\gamma}_s$ is the parametric matrix which is not changing. Hence the algorithm can be easily applied in real time iris defect detection.

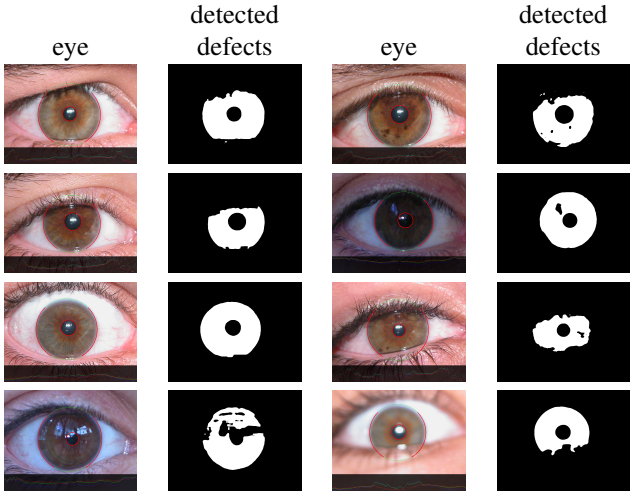

Figure 3. Eye images and the corresponding detected occlusions masks (even columns).

4. Experimental Results

The presented method was tested on the eye UBIRIS v1 and v2 databases [26] and compared with the best results achieved during the Noisy Iris Challenge Evaluation contest [23]. These databases provide eye images with or without different occlusion types (Fig.2), and thus are an useful resource for the evaluation iris recognition methods. The UBIRIS.v1 database contains 1877 images collected from 241 persons in two distinct sessions. The RGB 800×600, 24 bit images were captured with the Nikon E5700 camera and saved in the JPEG format. For the first image capture session, the enrollment, they tried to minimize noise factors, specially those relative to reflections, luminosity, and contrast, having installed the framework inside a dark room. In the second session they changed the capture location in order to introduce natural luminosity factor. This enabled the appearance of heterogeneous images with respect to reflections, contrast, luminosity, and focus problems.

Table 1. Performance criteria (a eyelid, b reflection, c eyelash).

UBIRIS [26]	type	FP [%]	FN [%]	TP+TN [%]
Img_1_1_1	bc	1.00	10.56	88.44
Img_1_2_1	abc	8.13	5.25	86.62
Img_2_1_1	abc	8.83	2.81	88.36
Img_2_2_1	abc	14.40	3.49	82.11
Img_3_1_1	abc	5.04	2.93	92.04
Img_3_2_1	abc	3.16	3.60	93.23
Img_4_1_1	abc	31.79	2.20	66.01
Img_4_2_1	abc	15.51	1.77	82.72
Img_5_1_1	abc	3.08	8.22	88.70
Img_5_2_1	bc	5.94	1.09	92.97
Img_6_1_1	abc	2.83	3.07	94.10
Img_6_2_1	abc	12.67	7.39	79.95
Img_7_1_1	abc	7.41	4.66	87.93
Img_7_2_1	abc	32.75	2.35	64.89
Img_8_1_1	ab	0.44	4.36	95.20
Img_8_2_1	b	1.52	3.33	95.15
Img_9_1_1	abc	11.17	0.91	87.93
Img_10_1_1	abc	4.40	1.96	93.64
Img_11_1_1	abc	4.05	4.91	91.03
Img_11_2_1	abc	6.42	2.24	91.34
Img_12_1_1	abc	1.11	8.57	90.32
Img_12_2_1	abc	0.81	6.46	92.73
Img_13_1_1	abc	11.01	2.46	86.53
Img_13_2_1	abc	30.93	1.16	67.91
Img_14_1_1	abc	8.41	5.93	85.66
Img_15_1_1	abc	0.18	6.08	93.74
Img_15_2_1	abc	13.05	3.90	83.05
Img_16_1_1	ab	12.85	5.74	81.40
Img_16_2_1	bc	13.45	2.37	84.19
Img_17_1_1	ab	9.84	3.68	86.48
Img_18_1_1	abc	4.46	5.00	90.54
Img_18_2_1	abc	24.19	3.70	72.11
Img_19_1_1	ab	0.11	2.53	97.36
Img_19_2_1	bc	12.81	4.47	82.72
Img_20_1_1	abc	9.27	2.48	88.25
Img_20_2_1	abc	18.94	0.18	80.87
overall perf.		9.78	3,94	86.38

Single iris occlusions (Fig.2) were recognized on the selected subset of twenty persons the UBIRIS.v1 database (Tab.1) containing one or a combination of several iris occlusions (a - eyelid, b - reflection, c - eyelash). Single Tab.1 columns contain false positive (FP), false negative (FN), and correct recognition (TP+TN) for single test images. The

ground truth masks for single occlusion types were hand made. All combined results presented (Fig.3 even columns) are presented with basic majority filtering only to demonstrate the basic method's performance. Fig.3 exhibits reliable defects detection which is clearly visible on the corresponding resulted thematic maps. All defects were detected using simple models with a causal neighbourhood containing 5 sites $(\eta = 3)$. Fig.3 bottom left indicates a type of highly defective iris texture. This example illustrates correct detection and localization of the most frequented iris occlusion by the presented method.

The UBIRIS.v2 database [25] contains 11102 images collected from 261 persons. The RGB 400×300, 24 bit images were captured with the Canon EOS 5D camera and saved in the TIFF format.

The presented method was also compared with the top eight results (from 97 participants) [31, 28, 7, 18, 14, 3, 17, 19] from the Noisy Iris Challenge Evaluation Contest (NICE.I) [23]. The contest was run on the UBIRIS.v2 database which contains highly noisy eye images. The participants had 500 training images and a disjoint test set of 500 images was used to measure the pixel-by-pixel agreement between the binary maps made by each participant and the ground-truth data, manually built by the NICE.I organizers.

Our method ranked third (Tab.2) closely behind the second method [28]. However, the winning algorithm [31] is very complex, time consuming and suffers with numerous experimentally set control parameters. Similarly the second ranked method [28] based on the reflections localization, reflections filling in, iris boundaries localization and eyelids boundaries localization steps, relies on several experimentally found parameters.

Table 2. Iris defect detection Noisy Iris Challenge Evaluation Contest [23] top eight results comparison.

Rank	Method	No. par.	Error
1	Tan et al. [31]	9	0.0131
2	Sankowski et al. [28]	6	0.0162
3	**presented method**	2	**0.0168**
4	Almeida [7]	5	0.0180
5	Li et al. [18]	4	0.0224
6	Jeong et al. [14]	3	0.0282
7	Chen et al. [3]	5	0.0297
8	Scotti & Labbati [17]	12	0.0301
9	Luengo-Oroz et al. [19]	7	0.0305

5. Conclusions

The majority of published iris defect detection methods do not use any multispectral information, while our method takes advantage of exploiting both multispectral as well as the spatial information simultaneously. The method is simple, extremely fast and robust in comparison with these top-ranking alternative methods. The presented method results are promising, most iris occlusions on the UBIRIS iris textures were correctly localized. Our method ranked third when evaluated on the the Noisy Iris Challenge Evaluation Contest from the 97 competing algorithms. The presented method can be easily generalized for gradually changing (e.g., illumination, colour, etc.) iris texture defect detection by exploiting its adaptive learning capabilities.

Acknowledgments

This research was supported by grant GAČR 102/08/0593 and partially by the grant GAČR 103/11/0335.

References

[1] F. H. Adler. *Physiology of the eye: clinical application*. The C.V. Mosby Co., St.Louis, 1959.

[2] K. W. Bowyer, K. Hollingsworth, and P. J. Flynn. Image understanding for iris biometrics: A survey. *Computer vision and image understanding*, 110(2):281–307, 2008.

[3] Y. Chen, M. Adjouadi, C. Han, J. Wang, A. Barreto, N. Rishe, and J. Andrian. A highly accurate and computationally efficient approach for unconstrained iris segmentation. *Image and Vision Computing*, 28(2):261 – 269, 2010.

[4] Y. Chen, S. C. Dass, and A. K. Jain. Localized iris image quality using 2-D wavelets. *Advances in Biometrics*, pages 0–6, 2005.

[5] D. Chetverikov. Detecting defects in texture. In *International Conference on Pattern Recognition*, pages 61–63, 1988.

[6] J. Daugman. High confidence visual recognition of persons by a test of statistical independence. *Pattern Analysis and Machine Intelligence, IEEE Transactions on*, 15(11):1148 –1161, Nov. 1993.

[7] P. de Almeida. A knowledge-based approach to the iris segmentation problem. *Image and Vision Computing*, 28(2):238 – 245, 2010.

[8] Y. Du, R. Ives, and D. Etter. A new approach to iris pattern recognition. *Proceedings of SPIE*, pages 1–12, 2004.

[9] H. Fujiwara, Z. Zhang, H. Toda, and H. Kawabata. Textile surface inspection by using translation invariant wavelet transform. In *IEEE Int. Symp. on Computational Intelligence in Robotics and Automation*, volume 3, pages 1427 – 1432. IEEE, IEEE, 2003.

[10] M. Haindl. Visual data recognition and modeling based on local markovian models. In L. Florack, R. Duits, G. Jongbloed, M.-C. Lieshout, and

L. Davies, editors, *Mathematical Methods for Signal and Image Analysis and Representation*, volume 41 of *Computational Imaging and Vision*, chapter 14, pages 241–259. Springer London, 2012. 10.1007/978-1-4471-2353-8_14.

[11] M. Haindl and S. Šimberová. *Theory & Applications of Image Analysis*, chapter A Multispectral Image Line Reconstruction Method, pages 306–315. World Scientific Publishing Co., Singapore, 1992.

[12] R. Haralick, K. Shanmugam, and I. Dinstein. Textural features for image classification. *Systems, Man and Cybernetics, IEEE Transactions on*, 3(6):610–621, 1973.

[13] Z. He, T. Tan, Z. Sun, and X. Qiu. Toward Accurate and Fast Iris Segmentation for Iris Biometrics. *Pattern Analysis and Machine Intelligence, IEEE Transactions on*, 31(9):1670–1684, Sept. 2009.

[14] D. S. Jeong, J. W. Hwang, B. J. Kang, K. R. Park, C. S. Won, D.-K. Park, and J. Kim. A new iris segmentation method for non-ideal iris images. *Image and Vision Computing*, 28(2):254 – 260, 2010.

[15] J. V. Kittler, R. Marik, M. Mirmehdi, M. Petrou, and J. Song. Detection of defects in colour texture surfaces. In *IAPR Workshop on Machine Vision Applications*, pages 558–567, 1994.

[16] A. Kumar. Inspection of surface defects using optimal fir filters. In *ICASSP*, volume II, pages 241–244. IEEE, 2003.

[17] R. D. Labati and F. Scotti. Noisy iris segmentation with boundary regularization and reflections removal. *Image and Vision Computing*, 28(2):270 – 277, 2010.

[18] P. Li, X. Liu, L. Xiao, and Q. Song. Robust and accurate iris segmentation in very noisy iris images. *Image and Vision Computing*, 28(2):246 – 253, 2010.

[19] M. A. Luengo-Oroz, E. Faure, and J. Angulo. Robust iris segmentation on uncalibrated noisy images using mathematical morphology. *Image and Vision Computing*, 28(2):278 – 284, 2010.

[20] R. Meylani, A. Ertuzun, and A. Ercil. A comparative study on the adaptive lattice filter structures in the context of texture defect detection. In *ICECS '96*, pages Vol II: 976 – 979, 1996.

[21] M. Mirmehdi, R. Marik, M. Petrou, and J. V. Kittler. Iterative morphology for fault detection in stochastic textures. *Electronic Letters*, 32:443–444, 1996.

[22] P. Mitra, C. Murthy, and S. Pal. Unsupervised feature selection using feature similarity. *IEEE Transactions on Pattern Analysis and Machine Intelligence*, 24(3):301–312, March 2002.

[23] H. Proena and L. A. Alexandre. Introduction to the special issue on the segmentation of visible wavelength iris images captured at-a-distance and on-the-move. *Image and Vision Computing*, 28(2):213 – 214, 2010.

[24] H. Proença and L. Alexandre. Iris recognition: Measuring feature's quality for the feature selection in unconstrained image capture environments. In *Computational Intelligence for Homeland Security and Personal Safety, Proceedings of the 2006 IEEE International Conference on*, pages 35–40. IEEE.

[25] H. Proenca, S. Filipe, R. Santos, J. Oliveira, and L. Alexandre. The ubiris.v2: A database of visible wavelength iris images captured on-the-move and at-a-distance. *Pattern Analysis and Machine Intelligence, IEEE Transactions on*, 32(8):1529 –1535, 2010.

[26] H. Proença and L. A. Alexandre. {UBIRIS}: A noisy iris image database. In *13th International Conference on Image Analysis and Processing - ICIAP 2005*, volume LNCS 3617, pages 970–977, Cagliari, Italy, 2005. Springer.

[27] H. Proença and L. A. Alexandre. A Method for the Identification of Noisy Regions in Normalized Iris Images. *18th International Conference on Pattern Recognition (ICPR'06)*, 4:405–408, 2006.

[28] W. Sankowski, K. Grabowski, M. Napieralska, M. Zubert, and A. Napieralski. Reliable algorithm for iris segmentation in eye image. *Image and Vision Computing*, 28(2):231 – 237, 2010.

[29] W. Sankowski, K. Grabowski, M. Zubert, and M. Napieralska. Iris Finder–Program For Reliable Iris Localization In Images Taken Under Visible Light. *Journal of Medical Informatics & Technologies Selected full texts*, 10:125–132, 2006.

[30] J. L. Sobral. Optimised filters for texture defect detection. In *International Conference on Image Processing*, volume III, pages 565–568, 2005.

[31] T. Tan, Z. He, and Z. Sun. Efficient and robust segmentation of noisy iris images for non-cooperative iris recognition. *Image and Vision Computing*, 28(2):223 – 230, 2010.

[32] R. P. Wildes. Iris recognition: an emerging biometric technology. *Proceedings of the IEEE*, 85(9):1348–1363, 1997.